

## A Structural Study of the Complexation of the Sodium Ion by the Cryptands 4,7,13,18-Tetraoxa-1,10-diazabicyclo[8.5.5]icosane and 4,7,13-Trioxa-1,10-diazabicyclo[8.5.5]icosane†

Stephen F. Lincoln,\* Ernst Horn, and Michael R. Snow

Department of Physical and Inorganic Chemistry, University of Adelaide, South Australia 5001

Trevor W. Hambley

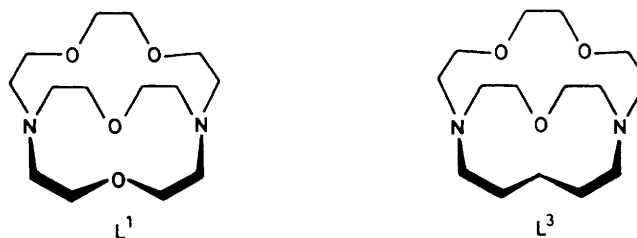
Department of Inorganic Chemistry, University of Sydney, New South Wales 2006

Ian M. Brereton and Thomas M. Spotswood

Department of Organic Chemistry, University of Adelaide, South Australia 5001

The crystal structures of the cryptates formed between sodium ion and 4,7,13,18-tetraoxa-1,10-diazabicyclo[8.5.5]icosane,  $[\text{Na}(\text{L}^1)(\text{NCS})]$ , and 4,7,13-trioxa-1,10-diazabicyclo[8.5.5]icosane,  $[\text{Na}(\text{L}^3)(\text{NCS})]$ , have been determined by single-crystal *X*-ray diffraction methods at 295 K and refined by least-squares methods to conventional *R* values of 0.069 and 0.039 for 1 417 and 2 259 reflections respectively. The respective crystals were of space group *Pcab* with  $a = 14.686(3)$ ,  $b = 15.699(4)$ ,  $c = 16.522(5)$  Å, and  $Z = 8$ ; and *P2<sub>1</sub>/n* with  $a = 9.947(2)$ ,  $b = 15.681(4)$ ,  $c = 12.460(3)$  Å,  $\beta = 95.27(2)^\circ$ , and  $Z = 4$ . Both  $[\text{Na}(\text{L}^1)(\text{NCS})]$  and  $[\text{Na}(\text{L}^3)(\text{NCS})]$  exist in the 'exclusive' form in which  $\text{Na}^+$  is located 0.14 and 0.37 Å respectively above the planes defined by the three oxygen atoms of the 15-membered cryptand rings. The  $^{13}\text{C}$  n.m.r. spectra of these cryptates are consistent with the retention of the exclusive structures in solution whilst the  $^{13}\text{C}$  n.m.r. spectra of the analogous  $\text{Li}^+$  cryptates indicate that they possess 'inclusive' structures in solution. Preliminary  $^{23}\text{Na}$  n.m.r. data show the rate of  $\text{Na}^+$  dissociation from  $[\text{Na}(\text{L}^1)]^+$  to be significantly less than that from  $[\text{Na}(\text{L}^3)]^+$  as indicated by dissociation rate constants (298.2 K) of  $12.1 \pm 0.2$  and  $(2.88 \pm 0.02) \times 10^4 \text{ s}^{-1}$  respectively determined in *N,N*-dimethylformamide solvent.

The polyoxadiazabicycloalkanes or cryptands<sup>1</sup> form cryptates with alkali metal ions ( $\text{M}^+$ ) in which  $\text{M}^+$  is totally inside the cryptand in an inclusive cryptate or in which  $\text{M}^+$  is located on the outside of a cryptand face in an exclusive cryptate. The inclusive cryptate is exemplified by  $[\text{Li}(\text{L}^1)]\text{I}$  ( $\text{L}^1 = 4,7,13,18$ -tetraoxa-1,10-diazabicyclo[8.5.5]icosane) and  $[\text{Na}(\text{L}^2)]\text{NCS}$  ( $\text{L}^2 = 4,7,13,16,21$ -pentaoxa-1,10-diazabicyclo[8.8.5]tricosane), and the exclusive cryptate by  $[\text{K}(\text{L}^2)(\text{NCS})]$ , whose structures have been determined by single-crystal *X*-ray diffraction methods.<sup>2,3</sup> {In the inclusive cryptates the  $\text{Li}^+$  and  $\text{Na}^+$  first co-ordination spheres are occupied solely by the binding groups of the cryptand whilst in the exclusive cryptate the nitrogen of  $\text{NCS}^-$  is within bonding distance of  $\text{K}^+$  and accordingly the above formulae are adopted for these cryptates. In solution both inclusive and exclusive cryptates are shown as cations,  $[\text{M}(\text{L})]^+$ , as any anion in the  $\text{M}^+$  first co-ordination sphere in the solid state is likely to be displaced by solvent on dissolution.} It has been deduced from  $^{13}\text{C}$  n.m.r. studies that these inclusive and exclusive structures are retained in solution and further that  $[\text{Na}(\text{L}^1)]^+$  exists as an exclusive cryptate in solution also.<sup>4-6</sup> Quite apart from its own intrinsic interest, a knowledge of the inclusive or exclusive nature of cryptates in solution can be important in mechanistic interpretation<sup>6</sup> of the kinetic parameters characterising  $\text{M}^+$  exchange between the fully solvated and the cryptate environment. As part of a wider structural and kinetic investigation of cryptates this study examines the structural effects of replacing an oxygen in one of the rings of  $\text{L}^1$  by a carbon to give 4,7,13-trioxa-1,10-diazabicyclo[8.5.5]icosane ( $\text{L}^3$ , shown schematically above) on the  $\text{Na}^+$  cryptate in the solid state by *X*-ray diffraction, and on



both  $\text{Na}^+$  and  $\text{Li}^+$  cryptates in solution by  $^{13}\text{C}$  n.m.r. spectroscopy; and in a preliminary way the effect on the lability towards exchange of  $\text{Na}^+$  between the fully solvated and cryptate environments in *N,N*-dimethylformamide (dmf) solution by  $^{23}\text{Na}$  n.m.r. spectroscopy.

### Experimental

**Materials.**— $\text{NaSCN}$ ,  $\text{LiSCN}$ , and  $\text{NaClO}_4$  were dried at 353–363 K under high vacuum for 48 h and were stored over  $\text{P}_2\text{O}_5$  under vacuum. *N,N*-Dimethylformamide was fractionally distilled from  $\text{CaH}_2$  under reduced pressure and stored over Linde 4A molecular sieves.  $\text{CDCl}_3$  and all other solvents were purified and dried by literature methods<sup>7</sup> and were stored over Linde 4A molecular sieves. Cryptand  $\text{L}^1$  (Merck) was distilled, dried under high vacuum for 24 h, and stored under dry nitrogen. Cryptand  $\text{L}^3$  has been discussed in the literature<sup>8</sup> but we were unable to find full experimental details of its preparation and accordingly the preparative method employed in this study, a modification of the general method of Lehn and co-workers,<sup>9</sup> is given in full. A solution of 1,4,10-trioxa-7,13-diazacyclopentadecane (Kryptofix-21, Merck) (2.0 g, 9.2 mmol) and triethylamine (2.5 g, 25.0 mmol) in dry benzene (100  $\text{cm}^3$ ), and a solution of pentanedioyl dichloride (1.41 g, 8.34 mmol) in

† Supplementary data available (No. SUP 56492, 8 pp.): H-atom coordinates, thermal parameters. See Instructions for Authors, *J. Chem. Soc., Dalton Trans.*, 1986, Issue 1, pp. xvii–xx. Structure factors are available from the editorial office.

dry benzene (100 cm<sup>3</sup>) were added simultaneously to dry benzene (1 200 cm<sup>3</sup>) over 8 h at 295 K with vigorous stirring under dry nitrogen using Perfusor motor-driven syringes. After filtration and removal of the solvent under vacuum the residue was chromatographed on 'flash' silica<sup>10</sup> [Merck, 230–400 mesh, methanol–dichloromethane (4:96),  $R_f = 0.30$ ], removal of the solvent and drying under high vacuum afforded the cryptand diamide as a white solid (2.2 g, 84%), m.p. 388–390 K;  $\nu_{\max}$ . 1 630, 1 130 cm<sup>-1</sup>; <sup>1</sup>H n.m.r. (CDCl<sub>3</sub>),  $\delta$  1.8–5.2, a complex spectrum with large peaks at 3.55 and 3.60 p.p.m.;  $m/e$  314 ( $M^+$ ), 286, 271, 246, 239, 28 (100). The diamide was reduced with borane–dimethyl sulphide as follows.<sup>11</sup> Diamide (1.3 g, 4.1 mmol) was dissolved in dry tetrahydrofuran (30 cm<sup>3</sup>) and treated with boron trifluoride etherate (1.0 cm<sup>3</sup>, 8.2 mmol) at 325 K under dry nitrogen. The reaction mixture was heated to reflux and borane–dimethyl sulphide (Fluka, 10% Me<sub>2</sub>S, 1.2 cm<sup>3</sup>, 10.9 mmol) was slowly added with a syringe. Heating was continued for 3 h and diethyl ether and Me<sub>2</sub>S distilled off as they formed. After allowing to cool to room temperature, solvent was removed under vacuum and the white residue was treated with 6 mol dm<sup>-3</sup> hydrochloric acid (25 cm<sup>3</sup>). The resultant solution was heated to reflux for 12 h and then evaporated to dryness. The crude cryptand was obtained from the hydrochloride salt after ion exchanging an aqueous solution on Dowex 1–8 × (OH<sup>-</sup> form, 50–100 mesh), concentration of the basic eluant, extraction with chloroform (4 × 50 cm<sup>3</sup>), and evaporation of the combined extracts. Distillation yielded L<sup>3</sup> (1.1 g, 92%) as a colourless oil (Found: C, 62.95; H, 10.55; N, 9.90. C<sub>15</sub>H<sub>30</sub>N<sub>2</sub>O<sub>3</sub> requires C, 62.9; H, 10.55; N, 9.80%). Accurate mass: found, 286.224 48; required,  $m/e$  286.225 628;  $m/e$  286 ( $M^+$ ), 269, 255;  $\nu_{\max}$ . 1 460m, 1 350m, 1 125s, 1 070m cm<sup>-1</sup>; <sup>1</sup>H n.m.r. (CDCl<sub>3</sub>),  $\delta$  1.35 (6 H, m, aliphatic –CH<sub>2</sub>–), 2.50 (12 H, m, –NCH<sub>2</sub>–), 3.40 p.p.m. (12 H, m, –OCH<sub>2</sub>–).

Crystals of [Na(L<sup>1</sup>)(NCS)] and [Na(L<sup>3</sup>)(NCS)] were prepared by dissolving equimolar amounts of NaSCN and the cryptand in dry methanol and evaporating to dryness. The white solids were dissolved in dry acetone and the solutions were then equilibrated with dry hexane in a desiccator whereupon white crystals slowly formed.

*X-Ray Crystallography of [Na(L<sup>1</sup>)(NCS)].—Crystal data.* C<sub>15</sub>H<sub>28</sub>N<sub>3</sub>NaO<sub>4</sub>S,  $M = 369.45$ , space group  $Pc\bar{a}b$ ,  $a = 14.686(3)$ ,  $b = 15.699(4)$ ,  $c = 16.522(5)$  Å,  $U = 3 809.2$  Å<sup>3</sup>,  $Z = 8$ ,  $D_m = 1.28$ ,  $D_c = 1.288$  g cm<sup>-3</sup>,  $F(000) = 1 584$ ,  $\lambda(\text{Mo-K}\alpha) = 0.7107$  Å,  $\mu(\text{Mo-K}\alpha) = 9.17$  cm<sup>-1</sup>.

*Data collection.* A crystal of dimensions 0.15 × 0.16 × 0.65 mm was mounted on a glass fibre and coated with cyanoacrylate 'super glue.' [The crystal density was measured by flotation in a mixture of CCl<sub>4</sub> and light petroleum (b.p. 373–393 K).] Lattice parameters were determined at 295 K by a least-squares fit to the setting angles of 25 independent reflections, measured and refined by scans performed on an Enraf-Nonius CAD 4 four-circle diffractometer employing graphite-monochromated Mo-K<sub>α</sub> radiation. Intensity data were collected in the range  $1.3 < \theta < 23^\circ$  using an  $\omega$ –( $n/3$ ) $\theta$  scan, where  $n$  (=1) was optimised by profile analysis of a typical reflection. The  $\omega$ –scan angles and horizontal apertures employed were  $(1.85 + 0.35\tan\theta)^\circ$  and  $(2.40 + 0.5\tan\theta)$  mm respectively. Three standard reflections, monitored after every 58 min of data collection, indicated that by completion of the data collection no decomposition had occurred. Data reduction and application of Lorentz and polarization corrections were performed using the program SUSCAD.<sup>12</sup> Of the 2 944 reflections collected 1 417 with  $I > 2.5\sigma(I)$  were considered observed and used in the calculations.

*Structure solution and refinement.* The structure was solved by direct methods using the routines for non-centrosymmetric solution of program SHELX.<sup>12</sup> The solution was confirmed as

being correct by analysis of the Patterson map. The thiocyanate ion, the sodium ion, and two oxygen atoms were located in the E-map. Least-squares refinement and calculation of a series of difference maps resulted in the location of a set of atoms with the expected connectivities. However at this stage the discrepancy index  $R$  had only converged to 0.19, some atoms had unacceptable large thermal parameters, and a number of peaks (*ca.* 2 e Å<sup>-3</sup> in height) remained in the difference maps. Therefore a model with the cryptate disordered was developed. In this model there are contributors to all oxygen and nitrogen sites but five carbon sites overlap which explains why initially not all atoms had large thermal parameters. A group multiplicity parameter, defining the disorder, refined to 0.60(1) and in the final refinement all atoms had reasonable thermal parameters. The shift associated with the disorder is small with all oxygen and nitrogen atoms lying *ca.* 1 Å from their images, and presumably arises as a consequence of the approximately spherical form of the cryptand. Only those atoms present at full occupancy were refined anisotropically. Hydrogen atoms for both contributors were included at sites calculated assuming tetrahedral geometry about carbon (C–H 0.97 Å). Full-matrix least-squares refinement converged (all shifts < 0.1 $\sigma$ ) with  $R = 0.069$ ,  $R' = 0.075$  and  $w = 5.33/[\sigma^2(F_o) + 0.000 44F_o^2]$ . The largest peak in a final difference map was 0.3 e Å<sup>-3</sup> in height. Final position parameters are listed in Table 1.

*X-Ray Crystallography of [Na(L<sup>3</sup>)(NCS)].—Crystal data.* C<sub>16</sub>H<sub>30</sub>N<sub>3</sub>NaO<sub>3</sub>S,  $M = 367.48$ , space group  $P2_1/n$ ,  $a = 9.947(2)$ ,  $b = 15.681(4)$ ,  $c = 12.460(3)$  Å,  $\beta = 95.27(2)^\circ$ ,  $U = 1 935.4$  Å<sup>3</sup>,  $Z = 4$ ,  $D_m = 1.25$ ,  $D_c = 1.261$  g cm<sup>-3</sup>,  $F(000) = 792$ ,  $\lambda(\text{Mo-K}\alpha) = 0.7107$  Å,  $\mu(\text{Mo-K}\alpha) = 1.69$  cm<sup>-1</sup>.

*Data collection.* A crystal of dimensions 0.08 × 0.16 × 0.28 mm was mounted on a glass fibre and coated with cyanoacrylate 'super glue.' The lattice parameters and the crystal density were determined as described above for [Na(L<sup>1</sup>)(NCS)]. Intensity data were collected in the range  $1.3 < \theta < 23^\circ$  using an  $\omega$ –( $n/3$ ) $\theta$  scan, where  $n$  (=1) was optimised by profile analysis of a typical reflection. The  $\omega$ –scan angles and horizontal apertures employed were  $(1.85 + 0.35\tan\theta)^\circ$  and  $(2.40 + 0.5\tan\theta)$  mm respectively. Three standard reflections, monitored after every 58 min of data collection, indicated that by completion of the data collection no decomposition had occurred. Data reduction and application of Lorentz and polarization corrections were performed using program SUSCAD.<sup>12</sup> Absorption corrections were applied with program ABSORB.<sup>12</sup> Maximum and minimum transmission factors were estimated to be 0.98 and 0.95 respectively. Of the 3 388 reflections collected 2 259 with  $I > 2.5\sigma(I)$  were considered observed and used in the calculations.

*Structure solution and refinement.* The sodium, oxygen, nitrogen, and most of the carbon atom locations were determined using the direct-method routine of the SHELX program.<sup>12</sup> The remaining carbon atoms were located in the Fourier difference maps of successive full-matrix least-squares refinements using the SHELX program. All hydrogen atoms were included at calculated positions (C–H 0.97 Å) assuming tetrahedral geometry about the carbon atoms and their thermal parameters were refined as a common group factor. In the final full-matrix least-squares calculations only the non-hydrogen atoms were modelled anisotropically. The refinement converged with  $R = 0.039$  and  $R' = 0.045$ . The weighting scheme employed converged at  $w = 2.90/(\sigma^2 F_o + 0.0002 F_o^2)$ . The largest peak remaining in the final difference map was associated with the O(2) atom and was less than 0.6 e Å<sup>-3</sup> in height. The final least-squares positional parameters are given in Table 2.

All the calculations pertaining to [Na(L<sup>1</sup>)(NCS)] and [Na(L<sup>3</sup>)(NCS)] were performed using the scattering for the respective neutral atoms from the International Tables.<sup>13</sup>

**Table 1.** Final positional parameters ( $\times 10^3$ ) for  $[\text{Na}(\text{L}^1)(\text{NCS})]^*$ 

Atom	x	y	z	Atom	x	y	z
Na(1)	6 035(2)	929(2)	2 263(2)	C(12)	4 151(9)	713(8)	1 356(9)
S(1)	7 463(2)	-1 287(2)	400(2)	C(13)	4 898(28)	927(28)	790(28)
O(1)	7 199(8)	1 050(8)	3 177(9)	C(14)	6 221(10)	1 700(11)	573(7)
O(2)	4 560(9)	440(7)	2 055(8)	C(15)	6 843(23)	2 157(29)	980(20)
O(3)	5 498(13)	1 553(11)	1 003(12)	O(1')	7 483(14)	1 286(12)	2 648(11)
O(4)	5 217(7)	2 369(6)	2 706(6)	O(2')	4 691(13)	258(10)	2 695(13)
N(1)	6 682(7)	-285(7)	1 583(7)	O(3')	4 847(28)	1 243(15)	1 391(15)
N(2)	5 337(10)	844(9)	3 626(7)	O(4')	5 902(26)	2 446(12)	2 876(13)
N(3)	7 026(14)	2 137(10)	1 837(12)	N(2')	6 040(29)	949(15)	3 746(13)
C(1)	7 010(7)	-692(6)	1 089(7)	N(3')	6 528(29)	2 064(15)	1 371(29)
C(2)	5 047(11)	1 682(10)	3 985(10)	C(2')	5 779(25)	1 805(29)	4 110(20)
C(3)	5 558(20)	2 455(28)	3 523(27)	C(3')	5 231(20)	2 370(20)	3 503(27)
C(4)	5 601(8)	3 014(7)	2 222(8)	C(5')	6 256(20)	2 934(28)	1 572(29)
C(5)	6 658(13)	2 973(12)	2 203(14)	C(6')	7 530(29)	1 904(27)	1 330(28)
C(6)	7 826(26)	1 821(15)	2 007(15)	C(7')	7 948(28)	1 882(27)	2 343(29)
C(7)	7 898(14)	1 606(13)	3 014(26)	C(8')	7 622(37)	1 364(23)	3 510(22)
C(8)	6 991(9)	872(8)	3 977(8)	C(10')	5 459(22)	208(20)	3 939(29)
C(9)	6 118(15)	433(14)	4 075(12)	C(12')	3 962(25)	519(21)	2 209(22)
C(10)	4 567(8)	256(7)	3 507(8)	C(14')	5 124(24)	1 480(38)	744(24)
C(11)	4 012(14)	522(11)	2 475(12)				

\* Primes denote the minor contributors to the disordered ligand.

**Table 2.** Final positional parameters for  $[\text{Na}(\text{L}^3)(\text{NCS})]^*$ 

Atom	x	y	z	Atom	x	y	z
Na(1)	76 782(11)	17 255(7)	44 974(10)	C(5)	7 069(4)	1 268(2)	1 545(3)
S(1)	76 287(10)	3 864(6)	82 118(8)	C(6)	5 751(3)	1 029(2)	2 002(3)
O(1)	8 397(2)	419(1)	3 944(2)	C(7)	6 034(3)	205(2)	3 679(3)
O(2)	8 565(3)	3 106(1)	4 667(2)	C(8)	7 401(3)	-167(2)	3 521(3)
O(3)	5 869(2)	2 693(1)	4 202(2)	C(9)	9 708(3)	301(2)	3 586(3)
N(1)	7 515(4)	1 298(2)	6 295(3)	C(10)	10 506(3)	1 101(2)	3 839(3)
N(2)	9 884(2)	1 871(2)	3 320(2)	C(11)	10 471(3)	2 651(2)	3 811(3)
N(3)	5 821(2)	1 050(2)	3 189(2)	C(12)	9 487(4)	3 347(2)	3 960(3)
C(1)	7 557(3)	914(2)	7 100(3)	C(13)	7 515(4)	3 701(2)	4 823(4)
C(2)	10 009(3)	1 855(2)	2 153(3)	C(14)	6 261(4)	3 554(2)	4 094(4)
C(3)	8 933(4)	2 372(2)	1 494(3)	C(15)	4 743(3)	2 434(2)	3 493(3)
C(4)	7 497(3)	2 178(2)	1 747(3)	C(16)	4 637(3)	1 481(2)	3 579(3)

\* Na and S co-ordinates  $\times 10^5$ , for the other atoms  $\times 10^4$ .**Table 3.** Bond lengths ( $\text{\AA}$ ) for  $[\text{Na}(\text{L}^1)(\text{NCS})]$ 

O(1)-Na(1)	2.289(14)	C(4)-O(4)	1.408(31)	O(1')-Na(1)	2.290(21)	C(8')-C(8)	1.430(39)
O(2)-Na(1)	2.324(13)	C(1)-N(1)	1.143(28)	O(2')-Na(1)	2.348(19)	C(10')-C(10)	1.493(73)
O(3)-Na(1)	2.433(19)	C(2)-N(2)	1.504(41)	O(3')-Na(1)	2.316(23)	C(12')-C(12)	1.469(81)
O(4)-Na(1)	2.662(9)	C(9)-N(2)	1.509(61)	O(4')-Na(1)	2.594(19)	C(14')-C(14)	1.672(86)
N(1)-Na(1)	2.409(11)	C(10)-N(2)	1.474(38)	N(2')-Na(1)	2.450(22)	C(7')-O(1')	1.264(40)
N(2)-Na(1)	2.478(13)	C(5)-N(3)	1.542(54)	N(3')-Na(1)	2.422(26)	C(8')-O(1')	1.443(43)
N(3)-Na(1)	2.492(17)	C(6)-N(3)	1.306(53)	C(1)-O(2')	1.355(46)	C(12')-O(2')	1.399(41)
C(1)-S(1)	1.616(28)	C(15)-N(3)	1.441(83)	C(12)-O(3')	1.319(58)	C(14')-O(3')	1.204(40)
C(8)-O(1)	1.385(18)	C(3)-C(2)	1.617(70)	C(4)-O(4')	1.469(49)	C(3')-O(4')	1.439(36)
C(7)-O(1)	1.374(59)	C(5)-C(4)	1.555(49)	C(8)-N(2')	1.455(27)	C(2')-N(2')	1.524(33)
C(11)-O(2)	1.402(56)	C(7)-C(6)	1.701(74)	N(3')-O(3)	1.817(69)	C(10')-N(2')	1.476(41)
C(12)-O(2)	1.370(38)	C(9)-C(8)	1.464(24)	C(6)-N(3')	1.496(39)	C(5')-N(3')	1.461(32)
C(13)-O(3)	1.365(70)	C(11)-C(10)	1.557(49)	C(14)-N(3')	1.506(72)	C(3')-C(2')	1.557(42)
C(14)-O(3)	1.299(42)	C(13)-C(12)	1.481(63)	C(5')-C(4)	1.448(62)	C(7')-C(6')	1.782(37)
C(3)-O(4)	1.447(62)	C(15)-C(14)	1.341(62)				

*N.M.R. Spectroscopy.*—Bruker WP-80 and CXP-300 n.m.r. spectrometers were used to run  $^{13}\text{C}$  and  $^{23}\text{Na}$  spectra at 20.2 and 79.39 MHz respectively. The broad band and selectively proton decoupled  $^{13}\text{C}$  spectra were run on anhydrous  $\text{CDCl}_3$  solutions (*ca.* 0.2 mol  $\text{dm}^{-3}$  in cryptand or cryptate at 305.2 K in a standard microprobe using a deuterium lock). An average of 30 000 transients was accumulated into a 16 384 point data base. The  $^{23}\text{Na}$  spectra were run on two dmf solutions,

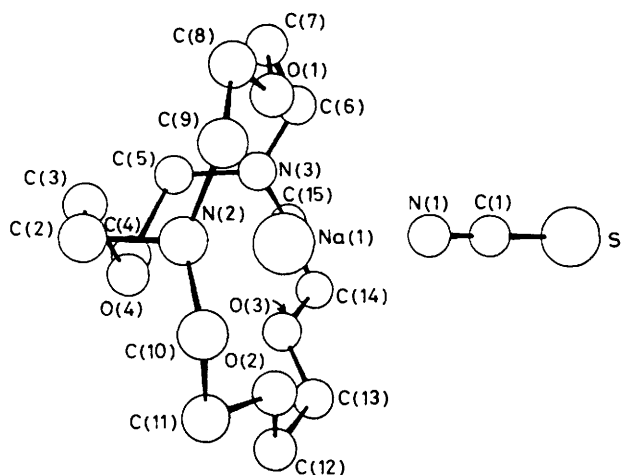
respectively 0.106 and 0.053, and 0.106 and 0.071 mol  $\text{dm}^{-3}$  in  $\text{NaClO}_4$  and  $\text{L}^3$ , prepared by weight from anhydrous materials in a dry nitrogen flushed glove-box and sealed under vacuum in 5-mm n.m.r. tubes. These tubes were coaxially inserted into 10-mm n.m.r. tubes containing  $(\text{CD}_3)_2\text{CO}$  which provided the deuterium lock frequency. An average of 6 000 transients was accumulated into a 2 048 data base at temperature intervals of 5 K over a temperature range of 215–300 K. The

**Table 4.** Valence angles (°) for [Na(L<sup>1</sup>)(NCS)]

N(1)–C(1)–S(1)	178.7(24)	C(3)–C(2)–N(2)	109.8(33)	C(8)–O(1)–C(7)	118.6(17)
C(1)–N(1)–Na(1)	160.4(11)	O(4)–C(3)–C(2)	102.1(38)	C(9)–C(8)–O(1)	113.1(13)
O(2)–Na(1)–O(1)	145.2(5)	C(4)–O(4)–C(3)	108.9(32)	C(8')–C(8)–N(2')	115.8(19)
O(3)–Na(1)–O(1)	140.7(6)	C(5)–C(4)–O(4)	112.4(25)	N(2')–C(10')–C(10)	111.3(25)
O(4)–Na(1)–O(1)	94.9(4)	C(5')–C(4)–O(4')	107.0(36)	C(10')–N(2')–C(8)	115.6(24)
O(3)–Na(1)–O(2)	72.8(6)	C(4)–C(5)–N(3)	113.2(35)	C(2')–N(2')–C(8)	102.1(21)
O(4)–Na(1)–O(2)	84.3(4)	C(15)–N(3)–C(5)	107.5(44)	C(2')–N(2')–C(10')	117.8(24)
O(4)–Na(1)–O(3)	75.4(5)	C(6)–N(3)–C(5)	123.6(49)	C(3')–C(2')–N(2')	112.3(24)
N(1)–Na(1)–O(1)	94.5(11)	C(15)–N(3)–C(6)	112.8(49)	O(4')–C(3')–C(2')	99.1(23)
N(1)–Na(1)–O(2)	92.2(4)	C(14)–C(15)–N(3)	127.5(59)	C(3')–O(4')–C(4)	112.1(17)
N(1)–Na(1)–O(3)	92.7(5)	C(15)–C(14)–O(3)	112.2(43)	N(3')–C(5')–C(4)	115.5(23)
N(1)–Na(1)–O(4)	168.1(4)	C(14')–C(14)–N(3')	102.6(45)	C(6')–N(3')–C(5')	114.8(21)
C(12)–O(2)–C(11)	113.9(34)	C(14)–O(3)–C(13)	121.0(45)	O(3')–C(14')–C(14)	122.7(33)
C(10)–C(11)–O(2)	109.5(35)	C(12)–C(13)–O(3)	118.6(48)	C(14')–O(3')–C(12)	114.7(31)
N(2)–C(10)–C(11)	110.0(25)	C(13)–C(12)–O(2)	106.1(33)	O(2')–C(12')–C(12)	117.8(29)
C(10')–C(10)–O(2')	110.8(35)	C(12')–C(12)–O(3')	103.6(44)	C(7')–C(6')–N(3')	107.4(22)
C(10)–N(2)–C(2)	112.5(27)	C(7)–C(6)–N(3)	110.0(42)	O(1')–C(7')–C(6')	101.8(21)
C(10)–N(2)–C(9)	112.4(32)	C(6)–C(7)–O(1)	105.8(38)	C(8')–O(1')–C(7')	104.9(26)
C(9)–N(2)–C(2)	113.4(31)				

**Table 5.** Bond lengths (Å) for [Na(L<sup>3</sup>)(NCS)]

O(1)–Na(1)	2.297(2)	C(9)–O(1)	1.429(4)	C(10)–N(2)	1.478(4)	C(5)–C(4)	1.504(5)
O(2)–Na(1)	2.340(3)	C(12)–O(2)	1.381(4)	C(11)–N(2)	1.465(4)	C(6)–C(5)	1.523(5)
O(3)–Na(1)	2.356(2)	C(13)–O(2)	1.427(4)	C(6)–N(3)	1.475(4)	C(8)–C(7)	1.509(4)
N(1)–Na(1)	2.358(4)	C(14)–O(3)	1.416(4)	C(7)–N(3)	1.466(4)	C(10)–C(9)	1.502(5)
N(2)–Na(1)	2.759(4)	C(15)–O(3)	1.421(4)	C(16)–N(3)	1.478(4)	C(12)–C(11)	1.490(5)
N(3)–Na(1)	2.576(3)	C(1)–N(1)	1.167(5)	C(3)–C(2)	1.522(5)	C(14)–C(13)	1.492(5)
C(1)–S(1)	1.609(5)	C(2)–N(2)	1.471(4)	C(4)–C(3)	1.522(5)	C(16)–C(15)	1.502(5)
C(8)–O(1)	1.416(4)						

**Figure 1.** Perspective view of [Na(L<sup>1</sup>)(NCS)]

sample temperature was controlled to  $\pm 0.3$  K with a Bruker B-VT 1000 variable-temperature unit and was monitored with a platinum resistance thermometer. The Fourier transformed spectra were subjected to complete lineshape analyses as previously described.<sup>6,14</sup>

## Results and Discussion

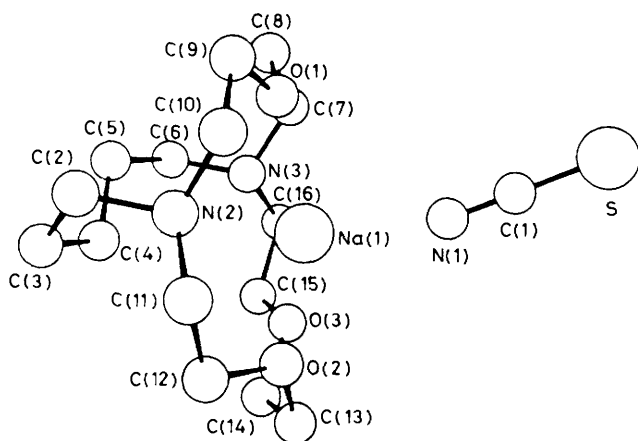
The bond lengths and bond angles for [Na(L<sup>1</sup>)(NCS)] are given in Tables 3 and 4 in which the primed atoms represent the minor contributors to the disordered cryptand.

The differences between the conformations of the primed and

unprimed cryptand are insignificant and the structure of the latter and major contributor is shown together with the atom numbering system in Figure 1. Thus [Na(L<sup>1</sup>)(NCS)] is seen to exist as an exclusive cryptate with Na<sup>+</sup> residing 0.14 Å outside the plane defined by O(1), O(2), and O(3) where the equation for the plane is  $-0.2705x + 0.8136y + 0.5146z = 0.6059$ . The [Na(L<sup>3</sup>)(NCS)] cryptate also exists as the exclusive complex as shown in Figure 2 which also shows the atom numbering system used for the bond lengths given in Table 5 and the bond angles in Table 6. In this cryptate Na<sup>+</sup> is 0.37 Å outside the plane defined by O(1), O(2), and O(3) (where the equation for the plane is  $-0.0725x + 0.2022y + 0.9767z = 3.3146$ ), a substantially greater distance than that observed in [Na(L<sup>1</sup>)(NCS)]. In both cryptates the large size of Na<sup>+</sup> relative to that of the cryptand cavity evidently dictates the formation of exclusive cryptates, in contrast to [Li(L<sup>1</sup>)]I which is an inclusive cryptate.<sup>2</sup> Complexation on the face of the 15-membered ring of both cryptands brings Na<sup>+</sup> into close proximity to three oxygens and two nitrogens. This together with the larger size of the cusp formed by this ring (and hence its greater ability to accommodate Na<sup>+</sup>), by comparison with that of the 12-membered ring, is probably the major determinant of stereochemistry in both exclusive cryptates. The closer proximity of Na<sup>+</sup> to the O(1), O(2), O(3) plane in [Na(L<sup>1</sup>)(NCS)] probably reflects the interaction of Na<sup>+</sup> with O(4) which is absent in [Na(L<sup>3</sup>)(NCS)]. In both cryptates N(1) of NCS<sup>-</sup> is within bonding distance of Na<sup>+</sup> and thus in [Na(L<sup>1</sup>)(NCS)] sodium is seven-co-ordinate [bonding interactions with O(1), O(2), O(3), O(4), N(1), N(2), and N(3)] whilst in [Na(L<sup>3</sup>)(NCS)] sodium is six-co-ordinate [bonding interactions with O(1), O(2), O(3), N(1), N(2), and N(3)]. As a consequence of the Na(1)–O(4) bonding interaction, a major stereochemical difference arises in the conformations of the C(2)–C(6) and C(2)–C(5) bridges of [Na(L<sup>3</sup>)(NCS)] and [Na(L<sup>1</sup>)(NCS)] respectively (Figures 1 and 2). Other

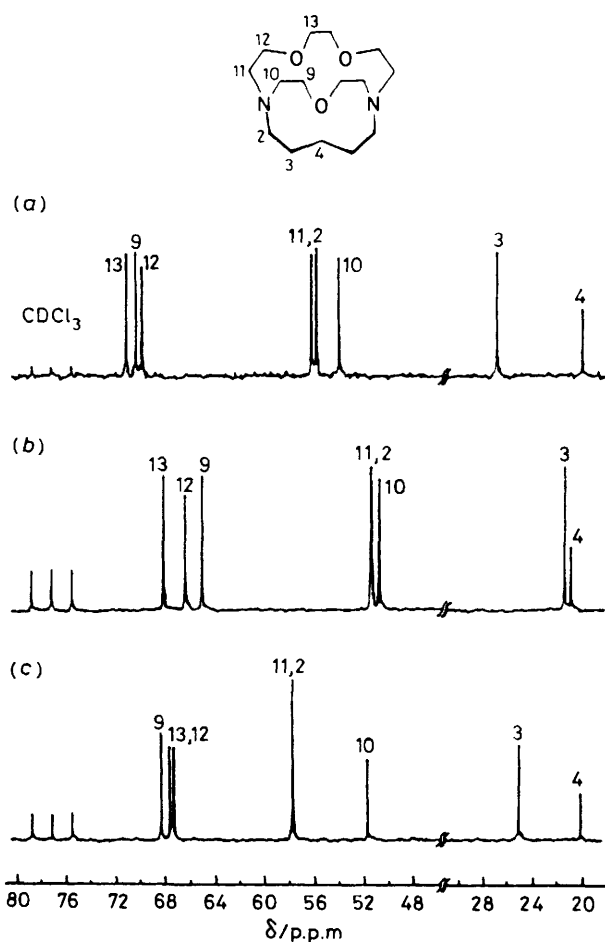
**Table 6.** Bond angles ( $^{\circ}$ ) for  $[\text{Na}(\text{L}^3)(\text{NCS})]$ 

N(1)–C(1)–S(1)	179.5(3)	C(10)–N(2)–C(2)	110.4(3)	C(8)–C(7)–N(3)	113.2(3)
C(1)–N(1)–Na(1)	164.3(3)	C(11)–N(2)–C(2)	111.1(3)	C(7)–C(8)–O(1)	107.9(3)
O(2)–Na(1)–O(1)	136.7(1)	C(7)–N(3)–C(6)	112.8(3)	C(10)–C(9)–O(1)	107.9(3)
O(3)–Na(1)–O(1)	141.4(1)	C(11)–N(2)–C(10)	111.4(3)	C(9)–C(10)–N(2)	113.4(3)
O(3)–Na(1)–O(2)	72.2(1)	C(16)–N(3)–C(6)	112.0(3)	C(12)–C(11)–N(2)	115.0(3)
N(1)–Na(1)–O(1)	94.7(1)	C(16)–N(3)–C(7)	111.5(3)	C(11)–C(12)–O(2)	111.2(3)
N(1)–Na(1)–O(2)	103.6(1)	C(3)–C(2)–N(2)	113.9(3)	C(14)–C(13)–O(2)	113.4(3)
N(1)–Na(1)–O(3)	102.3(1)	C(4)–C(3)–C(2)	114.1(3)	C(13)–C(14)–O(3)	108.1(3)
C(9)–O(1)–C(8)	115.3(2)	C(5)–C(4)–C(3)	114.3(3)	C(16)–C(15)–O(3)	107.3(3)
C(13)–O(2)–C(12)	116.4(3)	C(6)–C(5)–C(4)	114.3(3)	C(15)–C(16)–N(3)	111.6(3)
C(15)–O(3)–C(14)	114.9(3)	C(5)–C(6)–N(3)	114.0(3)		

**Figure 2.** Perspective view of  $[\text{Na}(\text{L}^3)(\text{NCS})]$ 

stereochemical differences are the larger Na(1)–N(1) distance and the smaller N(1)–Na(1)–O(2) and N(1)–Na(1)–O(3) angles observed for  $[\text{Na}(\text{L}^1)(\text{NCS})]$ .

The  $^{13}\text{C}$  n.m.r. spectra of  $\text{L}^3$  and its  $\text{Na}^+$  and  $\text{Li}^+$  cryptates in  $\text{CDCl}_3$  solution are shown in Figure 3; the associated chemical shifts, and those of  $\text{L}^1$  and its  $\text{Na}^+$  and  $\text{Li}^+$  cryptates, are given in Table 7. The resonances arising from  $\text{L}^3$  are in three distinct groups: those of carbons adjacent to oxygen [C(9), C(12), and C(13)], of carbons adjacent to nitrogen [C(2), C(10), and C(11)], and of carbons adjacent to carbon only [C(3) and C(4)]. The assignments of C(9), C(12), and C(13) are made by comparison to those made for  $\text{L}^1$  (as are those for the  $\text{Na}^+$  and  $\text{Li}^+$  cryptates),<sup>5,6</sup> and the assignments of C(3) and C(4) are obvious. In principle, selective decoupling of the C(3) protons should distinguish the C(2) resonance from those of C(10) and C(11) and similar decoupling of C(9) and C(12) should distinguish the resonances of C(10) and C(11) from that of C(2). In practice overlap of the proton coupled resonances of C(2), C(10), and C(11) rendered distinguishing between C(2) and C(11) a little uncertain for  $\text{L}^3$  and  $[\text{Li}(\text{L}^3)]^+$  but in the case of  $[\text{Na}(\text{L}^3)]^+$  the assignment of the superimposing C(2) and C(11) resonances is unambiguous. The decoupling experiments do not distinguish between C(10) and C(11) but as the C(10) resonance has been unambiguously assigned as appearing upfield of that of C(11) in the spectra of  $\text{L}^1$  and its  $\text{Na}^+$  and  $\text{Li}^+$  cryptates<sup>6</sup> it is unlikely that the relative chemical shifts of C(10) and C(11) will change in the very similar  $\text{L}^3$  and its alkali metal cryptates. The spectra in Figure 3 and Table 7 demonstrate that the changes in the chemical shifts of  $\text{L}^3$  caused by complexation of  $\text{Na}^+$  and  $\text{Li}^+$  differ significantly as is also the case for  $\text{L}^1$ . It is generally observed that complexation of  $\text{L}^4$  (= 4,7,13,16,21,24-hexaoxa-1,10-diazabicyclo[8.8.8]hexacosane) by  $\text{K}^+$ ,  $\text{Na}^+$ , and  $\text{Li}^+$ ;<sup>5</sup>  $\text{L}^2$  by  $\text{K}^+$ ,  $\text{Na}^+$ , and  $\text{Li}^+$ ;<sup>4,5</sup> and  $\text{L}^1$  by  $\text{Na}^+$  and  $\text{Li}^+$ <sup>5,6</sup> produces

**Figure 3.**  $^{13}\text{C}$  N.m.r. spectra (20.1 MHz) of (a)  $\text{L}^3$ , (b)  $[\text{Li}(\text{L}^3)]^+$ , and (c)  $[\text{Na}(\text{L}^3)]^+$  in  $\text{CDCl}_3$  solution at 305 K. The low-field triplet arises from  $\text{CDCl}_3$ . The resonance numbering corresponds to that in the structure shown and is identical to that shown for  $\text{L}^3$  in Figure 2

an upfield shift of the cryptand  $^{13}\text{C}$  resonances with the exception of the C(11) resonance of  $[\text{Na}(\text{L}^1)]^+$  and the equivalent resonance in  $[\text{K}(\text{L}^2)]^+$ . This distinguishes these two exclusive cryptates from the other cryptates which exist in the inclusive form. This difference in shift direction is also seen for the C(11) [and C(2)] resonances of  $[\text{Li}(\text{L}^3)]^+$  and  $[\text{Na}(\text{L}^3)]^+$  consistent with their existence as inclusive and exclusive cryptates respectively. The chemical shifts of C(3) and C(4) of  $[\text{Na}(\text{L}^3)]^+$  and  $[\text{Li}(\text{L}^3)]^+$  differ substantially, with those of the latter differing most from those of  $\text{L}^3$ . This is consistent with C(3) and C(4) in the inclusive  $\text{Li}^+$  cryptate being in close

**Table 7.**  $^{13}\text{C}$  N.m.r. chemical shifts\* for  $\text{L}^1$ ,  $\text{L}^3$  and their  $\text{Li}^+$  and  $\text{Na}^+$  cryptates at 305 K

Carbon	$\text{L}^1$	$[\text{Li}(\text{L}^1)]^+$	$[\text{Na}(\text{L}^1)]^+$	Carbon	$\text{L}^3$	$[\text{Li}(\text{L}^3)]^+$	$[\text{Na}(\text{L}^3)]^+$
12	70.752	68.717	69.021	13	71.298	68.383	67.897
11	70.053	66.986	67.624	12	70.053	66.683	67.594
3, 8	70.266	65.954	69.324	9	70.539	65.377	68.596
10	57.512	51.864	58.362	11	56.541	51.986	58.180
2, 9	55.690	50.619	54.901	2	56.146	51.864	58.180
				10	54.354	51.287	52.229
				3	27.693	22.409	25.841
				4	20.891	21.893	21.013

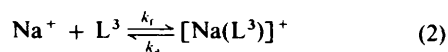
\* Chemical shifts are referenced to the centre peak of  $\text{CDCl}_3$  ( $\delta$  77.25 p.p.m.). The numbering system is that used in the structures shown in Figures 1 and 2. The cryptand and cryptate concentrations were  $0.21 \text{ mol dm}^{-3}$ .

proximity to  $\text{Li}^+$  and consequently experiencing a major change in environment whilst in the exclusive  $\text{Na}^+$  cryptate C(3) and C(4) are more distant from  $\text{Na}^+$  (Figure 1) and their environment is more similar to that in  $\text{L}^3$ .

In the temperature range 215–235 K the  $^{23}\text{Na}$  spectra of two dmf solutions respectively 0.106 and 0.053, and 0.106 and 0.071  $\text{mol dm}^{-3}$  in  $\text{NaClO}_4$  and  $\text{L}^3$  consist of a singlet arising from solvated  $\text{Na}^+$  downfield from the  $[\text{Na}(\text{L}^3)]^+$  singlet, consistent with  $\text{Na}^+$  exchange between these two environments [equation (1)] being at the slow-exchange limit of the n.m.r. time-scale.



Integration of the two singlet areas shows all of the cryptand to be complexed by  $\text{Na}^+$  consistent with an apparent stability constant  $K (=k_f/k_d) > 100 \text{ dm}^3 \text{ mol}^{-1}$  [equation (2)]. Above



235 K two singlets exhibit the broadening and coalescence to one singlet anticipated for  $\text{Na}^+$  exchange between the two  $\text{Na}^+$  sites, this becomes increasingly rapid as the temperature increases. These spectral changes were subjected to complete lineshape analyses<sup>14</sup> from which the site lifetime of  $[\text{Na}(\text{L}^3)]^+$  ( $\tau = 1/k_d$ ) was determined at intervals of ca. 5 K in the temperature range 238–290 K. Linear regression analyses of these data through the Eyring equation yield dissociation rate constants,  $k_d(298.2 \text{ K}) = (2.88 \pm 0.03) \times 10^4$  and  $(2.89 \pm 0.03) \times 10^4 \text{ s}^{-1}$ ;  $\Delta H^\ddagger = 40.1 \pm 0.2$  and  $40.0 \pm 0.2 \text{ kJ mol}^{-1}$ ;  $\Delta S^\ddagger = -25.1 \pm 0.8$  and  $-25.4 \pm 0.7 \text{ J K}^{-1} \text{ mol}^{-1}$  respectively for the two solutions described above. When the two  $\tau$  data sets are combined,  $k_d(298.2 \text{ K}) = (2.88 \pm 0.2) \times 10^4 \text{ s}^{-1}$ ;  $\Delta H^\ddagger = 40.0 \pm 0.1 \text{ kJ mol}^{-1}$ ;  $\Delta S^\ddagger = -25.3 \pm 0.5 \text{ J K}^{-1} \text{ mol}^{-1}$  are obtained (in all cases the quoted errors represent one standard deviation for the fit of the data to the Eyring equation) which compare with  $k_d(298.2 \text{ K}) = 12.1 \pm 0.2 \text{ s}^{-1}$ ;  $\Delta H^\ddagger = 83.5 \pm 0.5 \text{ kJ mol}^{-1}$ ;  $\Delta S^\ddagger = 55.8 \pm 1.2 \text{ J K}^{-1} \text{ mol}^{-1}$  for  $\text{Na}^+$  exchange in the  $[\text{Na}(\text{L}^1)]^+$  system in dmf solution.<sup>6</sup> The 2 000-fold greater lability of  $[\text{Na}(\text{L}^3)]^+$  towards dissociation is a consequence of its smaller  $\Delta H^\ddagger$ . This in turn is a consequence of there being one less oxygen binding group in  $\text{L}^3$  than in  $\text{L}^1$  and the resultant greater distance of  $\text{Na}^+$  from the three oxygen and two nitrogen binding groups of the 15-membered ring in  $[\text{Na}(\text{L}^3)]^+$ , as evidenced by  $\text{Na}^+$  being  $0.37 \text{ \AA}$  outside the plane delineated by the three oxygens compared to  $0.14 \text{ \AA}$  in

$[\text{Na}(\text{L}^1)]^+$ . (These distances apply to the solid state where  $\text{NCS}^-$  is within bonding distance of  $\text{Na}^+$ . In solution this interaction is replaced by a similar one with dmf such that the relative distances of  $\text{Na}^+$  outside the three-oxygen plane will be retained for the two exclusive cryptates and it is probable that the absolute distances will not change greatly either.) In the absence of accurate stability constant data  $k_f$  cannot be calculated and so a full mechanistic scheme for  $\text{Na}^+$  exchange cannot be postulated. Studies in progress show that the relative labilities of  $[\text{Na}(\text{L}^3)]^+$  and  $[\text{Na}(\text{L}^1)]^+$  towards dissociation are retained in a range of solvents, and determinations of  $K$  in dmf and other solvents are proceeding.

#### Acknowledgements

We thank the Australian Research Grants Scheme for supporting this research and Dr. E. H. Williams for invaluable assistance. The award of a Commonwealth Postgraduate Research Award (to I. M. B.) is gratefully acknowledged.

#### References

- 1 J.-M. Lehn, *Acc. Chem. Res.*, 1978, **11**, 49.
- 2 D. Moras and R. Weiss, *Acta Crystallogr., Sect. B*, 1973, **29**, 400.
- 3 F. Mathieu, B. Metz, D. Moras, and R. Weiss, *J. Am. Chem. Soc.*, 1978, **100**, 4412.
- 4 E. Schmidt, J.-M. Tremillon, J.-P. Kintzinger, and A. I. Popov, *J. Am. Chem. Soc.*, 1983, **105**, 7563.
- 5 L. Echegoyen, A. Kaifer, H. D. Durst, and G. W. Gokel, *J. Org. Chem.*, 1984, **49**, 688.
- 6 S. F. Lincoln, I. M. Brereton, and T. M. Spotswood, *J. Chem. Soc., Faraday Trans. 1*, 1985, 1623.
- 7 D. D. Perrin, W. L. F. Armarego, and D. R. Perrin, 'Purification of Laboratory Chemicals,' 2nd edn., Pergamon, Oxford, 1980.
- 8 J.-M. Lehn, *Neurosci. Res. Prog. Bull.*, 1976, **14**, 133; *Pure Appl. Chem.*, 1979, **51**, 979.
- 9 B. Dietrich, J.-M. Lehn, J. P. Sauvage, and J. Blanzat, *Tetrahedron*, 1973, **29**, 1629.
- 10 W. C. Still, M. Kahn, and A. Mitra, *J. Org. Chem.*, 1978, **43**, 2923.
- 11 H. C. Brown, S. Narasimhan, and Y. M. Choi, *Synthesis*, 1981, 996.
- 12 SUSCAD and ABSORB Data reduction programs for the CAD 4 diffractometer, M. L. Guss, University of Sydney, 1976; SHELX, Program for crystal structure determination, G. M. Sheldrick, University of Cambridge, 1976.
- 13 'International Tables for X-Ray Crystallography,' Kynoch Press, Birmingham, 1974, vol. 4, pp. 99–149.
- 14 S. F. Lincoln, *Prog. React. Kinet.*, 1977, **9**, 1.

Received 22nd February 1985; Paper 5/299